

Contents lists available at ScienceDirect

Environmental Pollution

journal homepage: www.elsevier.com/locate/envpol

Vegetation reflectance spectroscopy for biomonitoring of heavy metal pollution in urban soils[☆]

Kang Yu ^{a,*}, Maarten Van Geel ^b, Tobias Ceulemans ^b, Willem Geerts ^b, Miguel Marcos Ramos ^c, Cindy Serafim ^c, Nadine Sousa ^c, Paula M.L. Castro ^c, Pierre Kastendeuch ^d, Georges Najjar ^d, Thierry Ameglio ^e, Jérôme Ngao ^e, Marc Saudreau ^e, Olivier Honnay ^b, Ben Somers ^a

^a Department of Earth & Environmental Sciences, KU Leuven, 3001, Heverlee, Belgium

^b Department of Biology, KU Leuven, 3001, Heverlee, Belgium

^c Universidade Católica Portuguesa, CBQF, Centro de Biotecnologia e Química Fina, Laboratório Associado, Escola Superior de Biotecnologia, Rua Arquiteto Lobão Vital, 172, 4200-374, Porto, Portugal

^d Laboratoire des sciences de l'ingénieur, de l'informatique et de l'imagerie, Strasbourg University, Illkirch, France

^e Université Clermont Auvergne, INRA, PIAF, F-63000, Clermont Ferrand, France

ARTICLE INFO

Article history:

Received 26 May 2018

Received in revised form

7 September 2018

Accepted 9 September 2018

Available online 17 September 2018

Keywords:

Soil heavy metal contamination

Leaf functional trait

Vegetation reflectance spectroscopy

Red-edge position

Bio-indicator

ABSTRACT

Heavy metals in urban soils may impose a threat to public health and may negatively affect urban tree viability. Vegetation spectroscopy techniques applied to bio-indicators bring new opportunities to characterize heavy metal contamination, without being constrained by laborious soil sampling and lab-based sample processing. Here we used *Tilia tomentosa* trees, sampled across three European cities, as bio-indicators i) to investigate the impacts of elevated concentrations of cadmium (Cd) and lead (Pb) on leaf mass per area (LMA), total chlorophyll content (Chl), chlorophyll *a* to *b* ratio (Chl_a:Chl_b) and the maximal PSII photochemical efficiency (Fv/Fm); and ii) to evaluate the feasibility of detecting Cd and Pb contamination using leaf reflectance spectra. For the latter, we used a partial-least-squares discriminant analysis (PLS-DA) to train spectral-based models for the classification of Cd and/or Pb contamination. We show that elevated soil Pb concentrations induced a significant decrease in the LMA and Chl_a:Chl_b, with no decrease in Chl. We did not observe pronounced reductions of Fv/Fm due to Cd and Pb contamination. Elevated Cd and Pb concentrations induced contrasting spectral changes in the red-edge (690–740 nm) region, which might be associated with the proportional changes in leaf pigments. PLS-DA models allowed for the classifications of Cd and Pb contamination, with a classification accuracy of 86% (Kappa = 0.48) and 83% (Kappa = 0.66), respectively. PLS-DA models also allowed for the detection of a collective elevation of soil Cd and Pb, with an accuracy of 66% (Kappa = 0.49). This study demonstrates the potential of using reflectance spectroscopy for biomonitoring of heavy metal contamination in urban soils.

© 2018 Elsevier Ltd. All rights reserved.

[☆] This paper has been recommended for acceptance by Prof. Wen-Xiong Wang.
* Corresponding author. Division of Forest, Nature and Landscape, Department of Earth and Environmental Sciences, KU Leuven, Celestijnenlaan, 200e - box 2411, 3001, Leuven, Belgium.

E-mail addresses: kang.yu@kuleuven.be (K. Yu), maarten.vangeel@kuleuven.be (M. Van Geel), tobias.ceulemans@kuleuven.be (T. Ceulemans), willem.geerts@student.kuleuven.be (W. Geerts), mmramos@porto.ucp.pt (M.M. Ramos), cserafim@porto.ucp.pt (C. Serafim), nsousa@porto.ucp.pt (N. Sousa), plcastro@porto.ucp.pt (P.M.L. Castro), kasten@unistra.fr (P. Kastendeuch), georges.najjar@unistra.fr (G. Najjar), thierry.ameglio@inra.fr (T. Ameglio), jerome.ngao@inra.fr (J. Ngao), marc.saudreau@inra.fr (M. Saudreau), olivier.honnay@kuleuven.be (O. Honnay), ben.somers@kuleuven.be (B. Somers).

1. Introduction

Soil contamination is a widely spread problem across Europe (European Commission, 2006). Among the most frequent soil pollutants are heavy metals such as arsenic (As), cadmium (Cd), chromium (Cr), copper (Cu), mercury (Hg), lead (Pb), zinc (Zn), antimony (Sb), cobalt (Co) and nickel (Ni), which accumulate on the soil surface and transfer to deeper soil layers where they can infiltrate into the groundwater (Vince et al., 2014). Plants growing on heavy metal polluted soils passively take up heavy metals, jeopardizing their growth and negatively affecting other organisms

feeding on the plants (Panagos et al., 2013; Tóth et al., 2016). Furthermore, elevated concentrations of these heavy metals in agricultural or urban soils endanger food safety and public health (Poggio et al., 2009; Tóth et al., 2016).

Urban soils typically contain elevated concentrations of Cd, Cu, Zn and Pb, originating from anthropogenic activities such as traffic and industrial emissions (Gallagher et al., 2008; Li et al., 2001; Poggio et al., 2009; Pourkhabbaz et al., 2010; Vince et al., 2014). Cd and Pb are the most common heavy metals resulting from road traffic, which is attributed to the historical use of Pb as a gasoline additive (Kovarik, 2005) and Cd accumulation which is mainly due to abrasion of tires (Andersson et al., 2010; Vince et al., 2014). Cd and Pb are toxic for plants, animals and humans (Pandit et al., 2010; Poggio et al., 2009). Cd accumulates in human body and can cause nephropathy, pulmonary lesions and lung cancer after long period of exposure (Poggio et al., 2009). Pb increases blood pressure and damages liver, kidney and fertility, and most severely it reduces brain functioning and induces hyperactivity and hearing loss in children (Poggio et al., 2009). Therefore, it is vital to detect elevated concentrations of Cd and Pb in urban soils.

Measuring heavy metals is typically based on the collection of soil or road dust samples, which is labor intensive and costly, especially when monitoring heavy metal contamination at larger spatial scales (Wei and Yang, 2010). In European countries, the estimated total annual cost related to monitoring and remediating soil contaminants is 17.3 billion euros (European Commission, 2006), and around 81% of the expenditures is spent on remediation measures (Liedekerke et al., 2014). Consequently, only up to 15% is available to be spent on site investigations (Liedekerke et al., 2014), implying that there is a need for more cost-effective investigation methods to evaluate spatial and temporal heterogeneity of soil pollution. Soil near-infrared (NIR) spectroscopy has been applied for the detection of heavy metals at relatively low cost. However, this method requires intensive soil sampling (Pandit et al., 2010; Shi et al., 2014). Therefore, a spatially explicit characterization of heavy metal contamination at large scales is constrained by the capacity of sampling and sample processing, especially in urban areas characterized by sealed soil surfaces and highly heterogeneous land-use types.

Bio-indicators are living organisms that can be used to assess the quality of the environment (Holt and Miller, 2010; Parmar et al., 2016). Urban vegetation can be used as bio-indicators for monitoring air and soil pollution (Ho, 1990; Khavanin Zadeh et al., 2013; Sawidis et al., 2011). Plants concentrate metal elements in their above ground parts, which are indicative of elevated soil heavy metal concentrations. Furthermore, heavy metals can inhibit plant growth (Giulia et al., 2013; Horler et al., 1980), and decrease chlorophyll content and biomass productivity (Gallagher et al., 2008; Manios et al., 2003). Cd and Pb often limit plant growth by altering leaf internal structures (Giulia et al., 2013; Pourkhabbaz et al., 2010). For instance, Cd can reduce cell wall extensibility and relative water content (Barceló and Poschenrieder, 1990). Pb can reduce not only the leaf expansion but also the total chlorophyll content and efficiency of PSII electron transport (Kastori et al., 1998). Overall, heavy metal toxicity causes multiple direct and indirect effects on various physiological functions and on the morphology of plants (Barceló and Poschenrieder, 1990), reflected in changes of leaf functional traits.

Metal induced morphological and physiological changes can further alter vegetation absorbance and reflectance characteristics (Horler et al., 1980). Typically, heavy metal contamination induces most notable changes in the visible and NIR spectral regions, and thus reflectance spectroscopy holds great promise for evaluating the impact of heavy metal contamination on vegetation (Clevers et al., 2004; Kooistra et al., 2004, 2003; Rosso et al., 2005). By

applying reflectance spectroscopy to monitoring candidate bio-indicators located at multiple sites in urban areas, researchers have been able to detect polluted sites (Khavanin Zadeh et al., 2013). Previous studies have investigated the effect of individual metals on vegetation spectral responses, e.g., canopy reflectance in response to manipulated pot-soil Cd changes (Rosso et al., 2005). However, different metals may induce similar or contrasting spectral responses (Amer et al., 2017; Horler et al., 1980; Manios et al., 2003). Some studies have focused on spectral response in specific spectral bands such as the red-edge region (690–740 nm), which has been used to estimate plant chlorophyll variations under stress due to heavy metals (Clevers et al., 2004; Rosso et al., 2005). The red-edge position (REP) is defined as the position generating the maximum slope (inflection point) of the reflectance spectra (or maximum first derivative reflectance) in the red-edge region (Clevers et al., 2004; Horler et al., 1983), and has been found to be negatively related to soil Pb concentration (Clevers et al., 2004; Kooistra et al., 2004). Overall, associating soil heavy metal pollution with a range of plant functional and reflectance characteristics provides a cost-effective method for assessing heavy metal pollution. However, there is still a lack of vegetation reflectance spectroscopy studies that bio-monitor Cd and Pb contamination across a variety of urban environments, especially for monitoring contamination due to multiple metals.

Here we tested *Tilia tomentosa* as a bio-indicator for elevated soil Cd and Pb concentrations. Selecting 187 study trees across three European cities (Leuven, Porto and Strasbourg), our objectives were: i) to assess the impacts of elevated concentrations of Cd and Pb on leaf mass per area (LMA), total chlorophyll content (Chl), chlorophyll *a* to *b* ratio (Chl_a:Chl_b) and the maximal PSII photochemical efficiency (Fv/Fm); and ii) to investigate the feasibility of using leaf reflectance spectroscopy and partial-least-squares discriminant analysis for biomonitoring soil Cd and Pb contamination.

2. Materials and methods

2.1. Sampling of leaf and soil and heavy metal measurements

We conducted soil and leaf sampling in summer 2017 and randomly selected 19 sites and 187 *T. tomentosa* trees across three medium sized cities (Leuven (Belgium): $n = 64$; Porto (Portugal), $n = 67$; Strasbourg (France): $n = 56$). We randomly selected trees for sampling, and the trunk diameter ranged 5–130 cm. For each tree, we sampled the top soils (0–10 cm) at three random locations surrounding the trunk, and the three locations are mixed for metal measurements. We sampled 15 leaves at three random positions in each tree and stored the leaf samples in a cool box with ice. We performed soil sampling once, while leaf sampling was performed multiple times throughout the growing season for a subset of trees in Leuven and Strasbourg.

Heavy metal concentrations in the soil were measured by digesting 50 mg of dried and sieved soil with 7.5 ml concentrated hydrochloric acid and 2.5 ml concentrated nitric acid. The digested solution was diluted to 10 ml and measured with ICP-OES. For quality control of soil metal analysis, an internal soil standard was run parallel with the soil samples, which deviated less than 5% of the known composition. In this study, we focused on Cd and Pb, as these were the heavy metals that reached the toxicity thresholds (Table 1).

2.2. Identification of contamination based on soil heavy metal thresholds

Soil heavy metal contamination levels were identified based on

Table 1

Measured soil heavy metal content and the threshold values for classification of contamination. Cd and Pb were the major contaminants in this study, and Pb was the only metal that reached the highline and thus Pb contamination was classified into three sub-classes. Bold font highlights the metals which had a significant number of observations reaching the toxicity thresholds.

| Metal | Range (mg/kg) | Threshold (mg/kg) | Number of observations (n) | | | |
|------------|---------------|-------------------|----------------------------|--------------|------|------|
| | | | Class 0 | Class 1/Pb 1 | Pb 2 | Pb 3 |
| Cd | 0–3.9 | 1 | 294 | 39 | | |
| Pb* | 0–2170.8 | 60 | 132 | 201 | 180 | 17 4 |
| Co | 0–15.9 | 20 | 333 | 0 | | |
| Cr | 0–120.9 | 100 | 327 | 6 | | |
| Cu | 0–159.1 | 100 | 330 | 3 | | |
| Ni | 0–76.8 | 50 | 331 | 2 | | |
| Zn | 10–265.8 | 200 | 329 | 4 | | |

*, Pb contamination sub-levels: 1) Low contamination ($60 \leq \text{Pb} < 200$ mg/kg); 2) Medium contamination ($200 \leq \text{Pb} < 750$ mg/kg); 3) High contamination ($\text{Pb} \geq 750$ mg/kg).

published threshold standards (Tóth et al., 2016) released by the Ministry of the Environment, Finland (MEF, 2007). We grouped the samples into two classes - non-contaminated and contaminated, subjected to individual metals (Table 1). Soil samples and corresponding leaf spectral observations (Section 2.3) were grouped into four classes according to Pb contamination following the MEF standard (MEF, 2007). The four classes included class 0 being non-contaminated ($\text{Pb} < 60$ mg/kg), class 1 of low contamination ($60 \leq \text{Pb} < 200$ mg/kg), class 2 of medium contamination ($200 \leq \text{Pb} < 750$ mg/kg) and class 3 of high contamination ($\text{Pb} \geq 750$ mg/kg).

We also defined four contamination classes subjected to both Cd and Pb contamination by re-grouping of the Cd and Pb binary classes (Table S1), i.e., four Cd x Pb classes including the non-contaminated (class 0), Cd contaminated only (class 1), Pb contaminated only (class 2) as well as when both Cd and Pb are over the thresholds (class 3).

2.3. Leaf reflectance and functional traits

Leaf reflectance was measured using an ASD FieldSpec 3 spectroradiometer (ASD Inc., Longmont, CO, USA) connected to a Plant Probe and Leaf Clip Assembly (ASD Inc., Longmont, CO, USA). It allows for reflectance measurement in a spectral range of 350–2500 nm with a band width of 1 nm. Next, we measured the leaf maximal PSII photochemical efficiency (F_v/F_m , ratio of the variable fluorescence to the maximal fluorescence) using a chlorophyll fluorescence meter (Handy PEA, Hansatech Instruments Ltd., Pentney, UK), combined with a leaf clip that allows for dark adaption (25 min). Then, we measured the leaf area using a flatbed scanner, followed by oven dry for 3 days, allowing to determine leaf mass per area (LMA). In total, aggregated per tree and sampling time, collected leave samples allowed for further statistical analysis on a sample size of 333 for reflectance and functional traits. The 333 observations of reflectance spectra and functional traits were grouped into their contamination classes subjected to the soil heavy metal contamination classes as defined in Section 2.2.

A random subset of the leaf samples ($n = 53$) were used to determine the total chlorophyll (Chl) and carotenoid (Car) content. Leaf round discs with a diameter of 28.6 mm were punched from the leaf samples using a paper punch. Chla, Chlb and Car were extracted with a mortar and pestle in 80% acetone and their concentrations determined by measuring the solution absorbance (A) at wavelengths 470, 646.8 and 663.2 nm using a UV-VIS spectrophotometer (Shimadzu 1650 PC, Kyoto, Japan) according to Eqs. (1)–(3) (Lichtenthaler, 1987).

$$\text{Chla} = 12.25 * A_{663.2} - 2.79 * A_{646.8} \quad (1)$$

$$\text{Chlb} = 21.50 * A_{646.8} - 5.10 * A_{663.2} \quad (2)$$

$$\text{Car} = \frac{1000 * A_{470} - 1.82 * \text{Chla} - 85.02 * \text{Chlb}}{198} \quad (3)$$

For quality control of chlorophyll analysis, we performed parallel measurements in 12 samples, and the average standard error was lower than 5%.

2.4. Spectral and statistical analysis

To highlight the metal-induced spectral variations, we calculated the reflectance relative differences between group means for the contaminated and non-contaminated classes subjected to Cd and Pb contamination. We also applied first derivatives to the reflectance, focusing mainly on the red-edge region, to derive the red-edge inflection point (REIP) and evaluate the metal induced red-edge shifts (Clevers et al., 2004).

Partial least squares (PLS) regression is a multivariate method for relating two data matrices, X and Y, i.e., explanatory and response matrices, by extracting latent variables (components) to model the variations of both matrices (Wold et al., 2001). The PLS regression can reduce high dimensional data (e.g. hyperspectral) to a small number of latent variables which serve as new predictors on which the response variable is regressed (Rosipal and Krämer, 2006). Partial least squares discriminant analysis (PLS-DA) is a variant used when the response variable is categorical. We used PLS-DA for the classification of metal contamination classes. PLS-DA models were applied to four types of data, (i) the original reflectance spectral, and three pre-processed spectral data including (i) first derivative (ii), standard normal variate (SNV) and (iii) continuum removal (CR) precede applying the PLS-DA models. PLS-DA model calibration was first initiated on the entire dataset for the full spectrum with 10 components. The initial model was trained using a 10-fold cross-validation with 99 times of permutations, allowing for determination of the optimal number of components and the spectral bands yielding a variable importance in projection (VIP) ≥ 0.8 .

For an independent validation, the entire dataset was randomly split into the training and test subsets, with a sample size being 2/3 ($n = 215$) and 1/3 ($n = 118$) of the total observations ($n = 333$), respectively. The VIP ≥ 0.8 spectral bands were then used to train and test models on the two subsets, respectively.

PLS-DA Model classification accuracy was evaluated using the overall accuracy (Eq. (4)) and kappa coefficient (Eq. (5)), as well as for assessing the classification for individual classes using the producer's (Eq. (7)) and user's accuracies (Eq. (8)),

$$\text{Accuracy} = (TP + TN) / (TP + TN + FP + FN) \quad (4)$$

$$\text{Kappa} = \frac{p_a - p_e}{1 - p_e} \quad (5)$$

$$p_e = \frac{(TN + FP) \times (TN + FN) + (FN + TP) \times (FP + TP)}{(TP + TN + FP + FN)^2} \quad (6)$$

$$\text{Producer Accuracy} = TP / (TP + FN) \quad (7)$$

$$\text{User Accuracy} = TP / (TP + FP) \quad (8)$$

where the letters T and F denote true and false, respectively, and P

and N denote *positive* and *negative*, respectively, p_a is the actual agreement (identical to accuracy), whereas p_e is the expected agreement by chance (random accuracy) that can be calculated as Eq. (6).

We used linear mixed models to test whether elevated soil heavy metals affect the leaf functional traits. We defined the metal contamination classes, i.e., binary or multi-class, as the fixed effect factor and defined city and sampling site as random effect factors in the mixed models. All analyses were performed in the R programming environment (R Core Team, 2016). The R package ‘lme4’ (Bates et al., 2015) was used for running the mixed models, and the package ‘lsmeans’ (Lenth, 2016) was used for post-hoc analysis of pairwise comparisons between the contaminated classes based on Tukey’s test. PLS-DA was implemented using the package ‘mixOmics’ (Rohart et al., 2017).

3. Results and discussion

3.1. Heavy metal effects on leaf functional traits

Elevated Pb and Cd concentrations had a significant effect on LMA of *T. tomentosa* trees (Table 2). Soil Cd contamination did not induce significant changes in LMA (Fig. 1a), whereas Pb contamination significantly decreased LMA (Fig. 1b). Generally, Cd and Pb stress leads to damages to chloroplasts and thylakoid membranes in plants (Shen et al., 2016; Wu et al., 2014), which often causes reduced leaf growth such as small leaf size and small stomata (Shi and Cai, 2009), as well as thin cuticles of leaf surfaces (Pourkhabbaz et al., 2010). Therefore, elevated Pb concentrations could have reduced leaf thickness and thus decreased LMA. Cd also induces changes in leaf structural properties, while Cd concentrations measured in this study might still be below the threshold that induces significant inhibition of leaf expansion.

Elevated soil Pb induced significant changes in leaf total Chl content, Chla to Chlb ratio (Chla:Chlb) and Fv/Fm, whereas Cd and other metals did not yield significant changes (Table 2). Decrease in leaf Chl content is often associated with photoinhibition and reduction of the photosynthetic capacity (Shen et al., 2016). Chla:Chlb decreased significantly along with the increase in soil Pb concentration (Fig. 2), suggesting that Chla was more suppressed compared to Chlb (Nie et al., 2016). Similarly, a significant reduction of Chla:Chlb has been found in *Torreya grandis* (Shen et al., 2016) and *Typha latifolia* plants (Manios et al., 2003) treated with a high

concentration of Cd and Pb, suggesting increases in chlorophyll hydrolysis due to the toxic effect (Manios et al., 2003). Results may differ for different plant species, for instance in a greenhouse environment, Horler et al. (1980) observed a significant decrease of Chla:Chlb in pea leaves due to elevated Cd concentrations, but no changes following elevated Pb (Horler et al., 1980).

Cd and Pb contamination induced a decrease in Fv/Fm (Fig. 3a and b), whereas Fv/Fm appeared to be not sensitive to low-level Pb contamination (Fig. 3d), suggesting that Cd and Pb stress may induce photosynthesis inhibition. Similarly, Cd was found to affect Fv/Fm in the wetland plant species *Salicornia virginica* (Rosso et al., 2005) and in the turf grass species *Festuca arundinacea* Schreb (Huang et al., 2017). Generally, the observed decrease in Fv/Fm in plants subjected to Cd/Pb stress is associated with the photo-inhibition of PSII, as a result of the overproduction of reactive oxygen species (ROS) (Huang et al., 2017; Shen et al., 2016). However, a significant decrease in Fv/Fm may not always be observable if Cd/Pb concentration does not exceed a high threshold (Huang et al., 2017; Shen et al., 2016). Giulia et al. (2013) found that a high soil Pb concentration did not decrease Fv/Fm in *Q. ilex* plants, and they argued that these metals may not significantly alter functionality of the photosynthetic apparatus. Similarly, Shi and Cai (2009) reported that Fv/Fm was not affected in peanut plants treated with a high concentration of Cd. Therefore, the effect of heavy metals on Fv/Fm might depend largely on metal type, concentration and plant species.

Mixed models for multi-class Cd×Pb and Pb contamination showed much more pronounced effects on LMA and Chla:Chlb than on Fv/Fm and leaf total Chl content (Table 3), which suggests that heavy metals induced more structural changes and proportional changes in leaf biochemicals than the quantity changes of individual components. An increase in leaf total Chl content and Fv/Fm was observed at a relative low-level Pb or Cd × Pb contamination (Table 3), suggesting that heavy metals impose complicated effects on photosynthesis and that Cd and Pb may increase the PSII quantum yield within a certain range of low concentrations (Ouyang et al., 2012; Shen et al., 2016).

The effect of soil heavy metals on leaves or the content of heavy metal accumulation in the leaves might be related to the age of trees (Doganalr et al., 2012). To test whether tree age difference affect the observed effects of Cd and Pb on leaf functional traits in this study, we used trunk diameter as a proxy of tree age and added it as an additional random factor in the mixed models (Table S2 and

Table 2

Results of mixed models for testing the effect of soil heavy metals on leaf functional traits, including the leaf mass per area (LMA), Fv/Fm, total chlorophyll content (Chl) and Chla:Chlb ratio. Modeled random effects were city and sites. Chlorophyll data were only available for a subset of the samples, where only Cd and Pb reached the thresholds of contamination. Bold font highlights the statistical significance of each test ($p < 0.05$).

| Mixed Model | | | | Tukey's Test Class 0–1 | |
|-------------|-------|---------|------------------|------------------------|------------------|
| Trait | Metal | F-value | P-value | Estimate | P-value |
| LMA | Cd | 1.11 | 0.292 | 0.249 | 0.292 |
| | Cr | 6.68 | 0.010 | –1.319 | 0.010 |
| | Cu | 0.16 | 0.691 | 0.284 | 0.691 |
| | Ni | 0.23 | 0.632 | 0.425 | 0.632 |
| | Pb | 67.08 | <0.001 | 1.284 | <0.001 |
| | Zn | 0.70 | 0.404 | 0.521 | 0.404 |
| Fv/Fm | Cd | 0.02 | 0.901 | –0.0013 | 0.901 |
| | Cr | 0.01 | 0.905 | 0.0027 | 0.905 |
| | Cu | 0.01 | 0.911 | 0.0034 | 0.911 |
| | Ni | 0.08 | 0.772 | –0.0109 | 0.772 |
| | Pb | 5.84 | 0.016 | –0.0162 | 0.016 |
| | Zn | 0.08 | 0.784 | –0.0074 | 0.784 |
| Chl | Cd | 2.31 | 0.138 | 18.091 | 0.138 |
| | Pb | 6.78 | 0.013 | –9.238 | 0.013 |
| Chla:Chlb | Cd | 0.45 | 0.509 | 0.181 | 0.509 |
| | Pb | 23.58 | <0.001 | 0.331 | <0.001 |

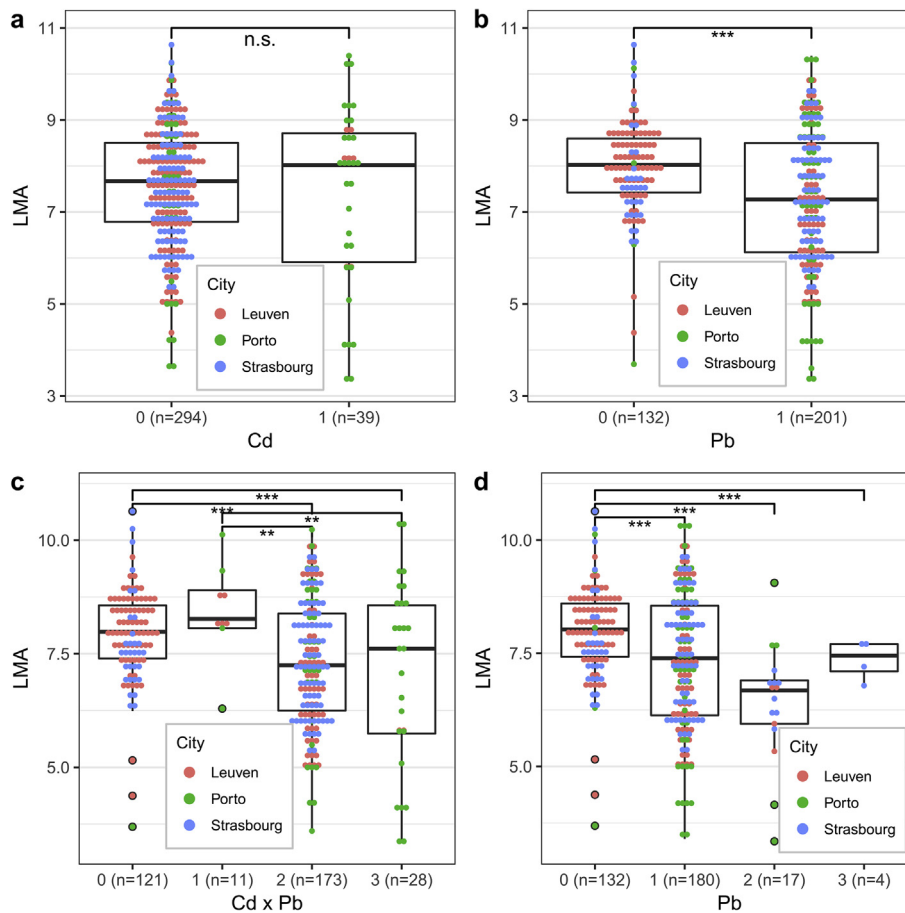


Fig. 1. Boxplots with the leaf mass per area (LMA) differences between the binary classes (0 = non-contaminated, 1 = contaminated) of (a) Cd and (b) Pb contamination, as well as among multiple classes of (c) Cd \times Pb and (d) Pb contamination. Significance levels are indicated according to the post-hoc Tukey's test of the applied mixed models.

Table S3). Results suggest that the observed effects of Cd and Pb on *T. tomentosa* leaves was not significantly influenced by tree age.

3.2. Reflectance and first derivatives in response to heavy metals

Elevated soil Cd concentrations yielded relatively large variations in leaf reflectance centered at the 500, 680 and 720 nm bands (Fig. 4a), whereas elevated Pb yielded large variations at the 550 and 700 nm bands (Fig. 4b). In the red-edge region, Cd had a large effect on reflectance at the red-edge center (~720 nm), whereas Pb had a large effect on reflectance ranging from the red absorption to the beginning of the red-edge bands (680–700 nm). Over the full spectrum, soil Pb contamination induced larger variations ($\pm 10\%$, Fig. 4b) compared to Cd contamination ($\pm 5\%$) (Fig. 4a), which might be attributed to the fact that Pb contamination was severer than Cd in this study. Cd concentration was slightly higher than the threshold (1 mg/kg), but was much lower than the 'low guideline' of contamination level (10 mg/kg) at which ecological or health risks present (Tóth et al., 2016).

The decrease in the NIR region (750–1400 nm) was associated with elevated Cd and Pb concentrations. This might be attributed partly to the decreased LMA because contaminated trees often have a much thinner outer epidermal layer and thus thinner leaves (Pourkhabbaz et al., 2010), although the effect of Cd on LMA observed in this study was marginal (Fig. 1). Metal-induced decreases in leaf NIR reflectance might be associated mainly with the changes in leaf internal structural properties which decrease the internal light scattering and increase the transmittance of leaves

(Horler et al., 1980; Kumar et al., 2001).

The first derivative reflectance in the visible-to-NIR bands showed two major peaks centered at 530 and 720 nm (Fig. S1). In the red-edge spectral region, Cd contamination induced a shift of absorbance features towards the shorter wavelengths (Fig. S1a). In contrast, Pb contamination induced a red-edge shift to the longer wavelengths (Fig. S1b). In addition to the red-edge bands, Pb contamination also yielded large variations in the first derivative reflectance at the green bands, suggesting a more pronounced change of the overall shape of reflectance (cf. Fig. 4). As shown in the first derivative reflectance, Pb contamination also induced a shift in the green edges (both sides of the green peak) compared to Cd contamination. This might explain the observed decrease in the Chla:Chlb ratio (Fig. 2), since absorption at the green edge bands is related to Chlb variations (Kumar et al., 2001).

The extracted REIP showed contrasting changes in the Cd and Pb contaminated trees, with decreasing and increasing trends, respectively (Fig. S2), which confirms the contrasting effects of Cd and Pb contamination on the red-edge reflectance. Heavy-metal induced REIP changes, or red-edge shifts, have been found to depend to some degree on plant species and sampling sites (Kooistra et al., 2004). Normally, a decreased REIP can be observed when plant stress induces a reduction in leaf total Chl content (Horler et al., 1983). However, here we did not observe obvious Chl reduction associated with Cd or Pb contamination. Therefore, the REIP variations observed here were more likely associated with the proportional changes in the Chla:Chlb ratio, in combination with changes in leaf structures.

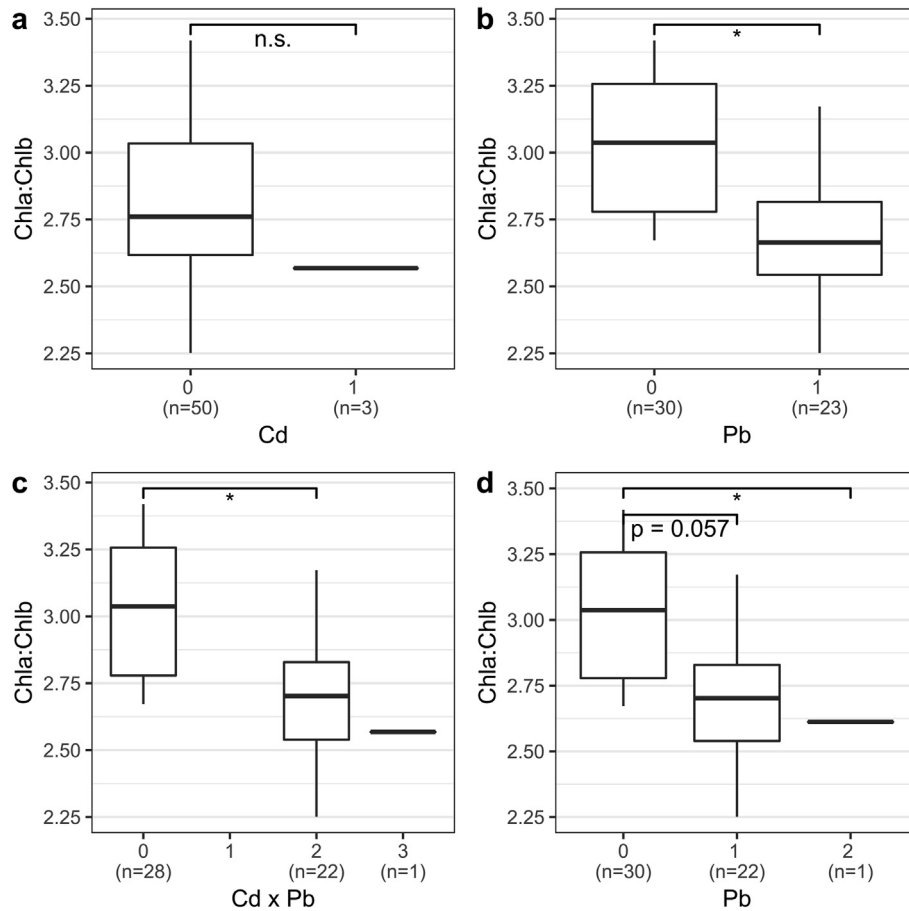


Fig. 2. Boxplots with the leaf chlorophyll *a* to *b* ratio (Chla:Chlb) differences between the binary classes (0 = non-contaminated, 1 = contaminated) of (a) Cd and (b) Pb contamination, as well as among multiple classes for (c) Cd × Pb and (d) Pb contamination. Significance levels are indicated according to the post-hoc Tukey's test of the applied mixed models.

3.3. PLS-DA model calibration for binary and multi-class classifications

In the binary classifications, the PLS-DA calibration models for Cd-contamination classification yielded a total accuracy of 84.1–86.5% ($\kappa = 0.46$ – 0.49 , Table S4). PLS-DA models for Pb contamination yielded a total accuracy of 72.7–77.8% ($\kappa = 0.46$ – 0.57). For the multi-class classification of Cd×Pb-mixed contamination, PLS-DA models yielded a total accuracy of 43.2–66.1% ($\kappa = 0.24$ – 0.49 , Table S4). PLS-DA models for the multi-class classification of Pb yielded a total accuracy of 52.0–64.0% ($\kappa = 0.29$ – 0.43). The best classifications for individual metals are illustrated in confusion-matrix plots (Fig. 5).

The best model for Cd correctly classified the Cd class 0 with a producer and use accuracy of 86% and 97%, respectively, and were 77% and 43% for the Cd class 1 (Fig. 5a). The producer and use accuracy for the Pb class 0 were 88% and 67%, respectively, and 77% and 90% for the Pb class 1 (Fig. 5b). The best model for Cd × Pb yielded a relatively low user accuracy in predicting the classes 1 and 3 (Fig. 5c), which however, accounts for a very small proportion of the total observations. The best model for multi-class Pb contamination yielded a relatively high producer accuracy for the classes 0 and 3 (Fig. 5d), with 80% and 100%, respectively. In contrast, the model yielded a higher user accuracy for the classes 0 and 1 than for the classes 2 and 3. The low user accuracy for the Pb classes 2 and 3 was mainly due to the small sample size of high Pb concentrations, which consists of only 17 and 4 observations for the

classes 2 and 3, respectively.

Overall, the high producer accuracy, paired with relatively low user accuracy for a relatively high metal concentration was rather encouraging, since our models slightly tended to overestimate the observed contamination rather than underestimate the elevated contamination. This implies a high probability of detecting the elevated concentrations of soil heavy metals.

3.4. PLS-DA model validation using full spectrum and VIP-bands

Compared to model calibration accuracies, model validation based on the full spectrum produced comparable accuracies (Table S5). In binary classifications, models for Pb contamination yielded higher κ coefficients than the models for Cd contamination. In multi-class classifications, model validation showed improved total accuracies and κ coefficients (Table S5), suggesting the potential of using calibrated PLS-DA models for detecting elevated soil Cd and Pb concentrations.

Validation of models trained with the VIP (≥ 0.8) bands showed slightly improved κ values and total accuracies compared to the full use of bands (Table S5). The importance of individual spectral bands in the classification is indicated by the VIP scores for individual metals (Fig. 6). Cd contamination yielded relatively high VIP scores at the red-edge (730 nm) and SWIR bands (1300 nm, 1650 nm) compared to Pb contamination, suggesting unique spectral responses to elevated soil Cd in these bands (Fig. 6). Pb contamination yielded higher VIP scores at the green (530 nm) and

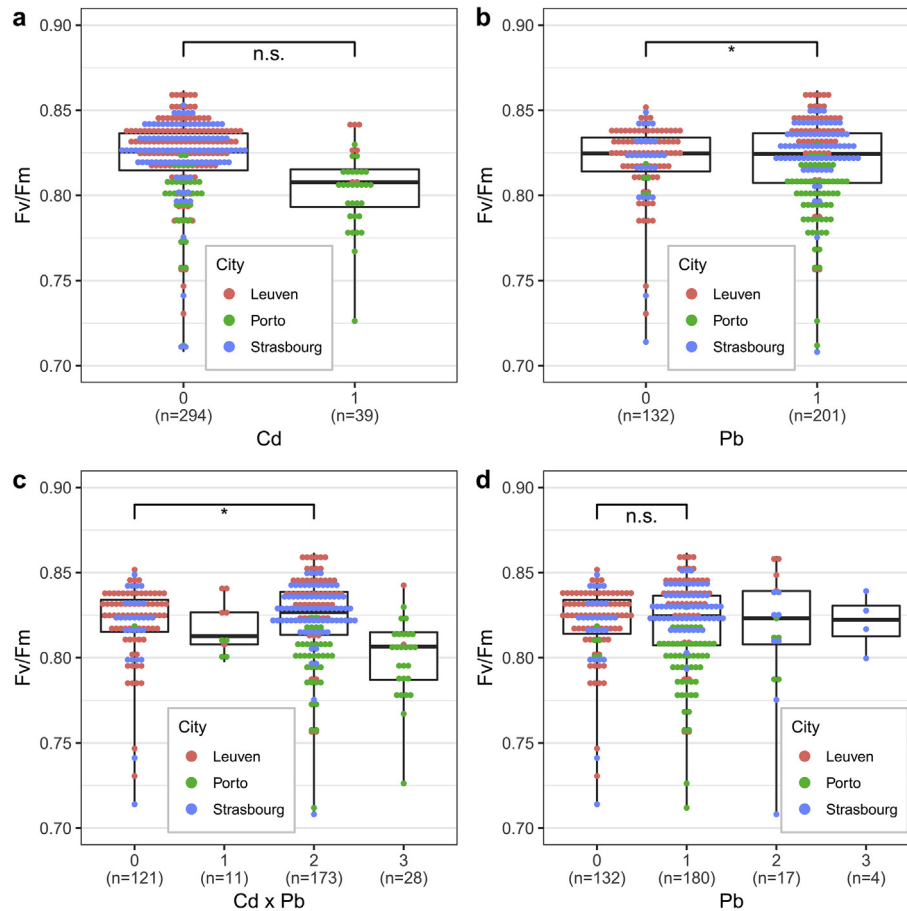


Fig. 3. Boxplots show the chlorophyll fluorescence Fv/Fm differences between the binary classes (0 = non-contaminated, 1 = contaminated) of (a) Cd and (b) Pb contamination, as well as among multi-class classifications of (c) Cd × Pb and (d) Pb contamination. Significance levels are indicated according to the post-hoc Tukey's test of the applied mixed models.

Table 3

Mixed models for testing the effect of multi-level Cd × Pb and Pb contamination on leaf functional traits, including the leaf mass per area (LMA), Fv/Fm, total chlorophyll content (Chl) and Chla:Chlb ratio. The modeled random effects are city and site. Chlorophyll data were only available for a subset of the samples, where only Cd and Pb reached the threshold of contamination. Bold font highlights the statistical significance of each test ($p < 0.05$).

| Mixed model | | | | Tukey's Test | | | | | | | | | | | |
|-------------|---------|---------|--------------|--------------|--------|-----------|--------------|-----------|--------|-----------|--------------|-----------|--------------|-----------|-------|
| Trait | Metal | F-value | P-value | Class 0–1 | | Class 0–2 | | Class 0–3 | | Class 1–2 | | Class 1–3 | | Class 2–3 | |
| | | | | estimate | p | estimate | p | estimate | p | estimate | p | estimate | p | estimate | p |
| LMA | Cd × Pb | 23.74 | <0.001 | 0.025 | 1.000 | 1.256 | <0.001 | 1.722 | <0.001 | 1.231 | 0.006 | 1.698 | 0.001 | 0.466 | 0.246 |
| | Pb | 26.29 | <0.001 | 1.21 | <0.001 | 1.831 | <0.001 | 2.444 | <0.001 | 0.621 | 0.104 | 1.234 | 0.104 | 0.613 | 0.731 |
| Fv/fm | Cd × Pb | 2.42 | 0.066 | −0.0211 | 0.661 | −0.0184 | 0.044 | −0.0143 | 0.713 | 0.0028 | 0.999 | 0.0069 | 0.987 | 0.0041 | 0.987 |
| | Pb | 2.00 | 0.113 | −0.0168 | 0.070 | −0.0109 | 0.863 | −0.0106 | 0.980 | 0.0059 | 0.971 | 0.0062 | 0.996 | 0.0003 | 1.000 |
| Chl | Cd × Pb | 5.86 | 0.006 | | | −10.275 | 0.014 | 12.558 | 0.495 | | | | | 22.834 | 0.108 |
| | Pb | 6.40 | 0.004 | −8.108 | 0.057 | −32.96 | 0.012 | | | −24.852 | 0.070 | | | | |
| Chla:Chlb | Cd × Pb | 11.47 | <0.001 | | | 0.332 | <0.001 | 0.319 | 0.319 | | | | | −0.012 | 0.998 |
| | Pb | 12.01 | <0.001 | 0.323 | <0.001 | 0.495 | 0.072 | | | 0.172 | 0.709 | | | | |

the beginning of red-edge (700 nm), suggesting that Pb contamination induced more pronounced responses in the visible bands. For the binary classifications, VIP-based PLS-DA models yielded higher accuracies for Pb-contamination classification ($\kappa = 0.66$) than for Cd ($\kappa = 0.39$, Table S5). For multi-class classifications, the VIP-based PLS-DA models yielded comparable accuracies by using a much less amount of bands compared to the use of full spectral bands.

Model validation results showed that selecting a set of influential bands ($VIP \geq 0.8$) allowed for maintaining classification accuracy and improving model-use and computational efficiencies.

Within a limited number of observations, by randomly dividing independent training and testing subsets of observations, our results suggest that spectrally calibrated PLS-DA models have great potential of applying to future scenarios for monitoring heavy metals.

3.5. Comparison between reflectance pre-processing methods

The kappa coefficient is a balanced measure compared to the use of the producer-, user- and total accuracies, especially when the observations in difference classes are highly imbalanced such as in

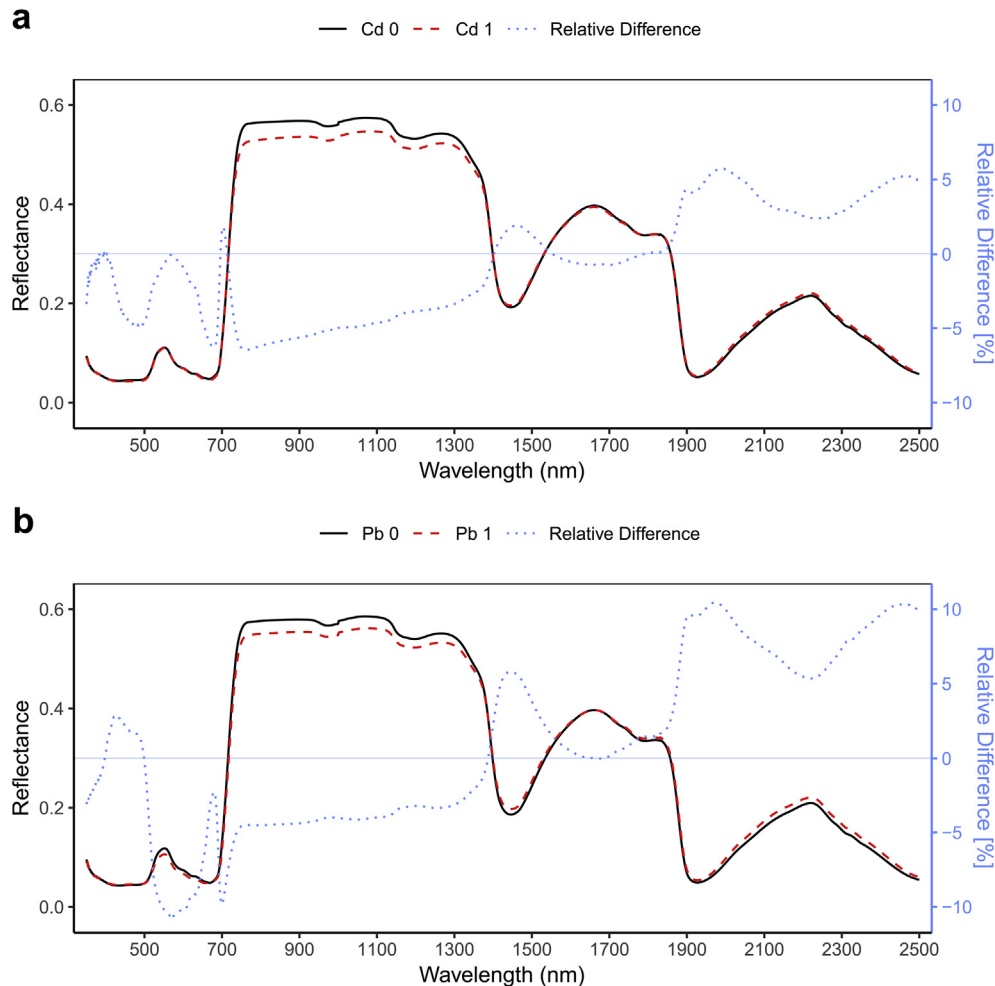


Fig. 4. Leaf mean reflectance of the contaminated (1) and non-contaminated (0) trees subjected to (a) Cd and (b) Pb, and their reflectance relative difference $((X_1 - X_0)/X_0)$ between the contaminated and non-contaminated leaves.

this study. Hence, we evaluated the three spectra-preprocessing methods according to the kappa values. Model calibration and validation both showed that the first derivatives yielded the highest kappa values compared to the use of the original and SNV reflectance data (Table S4 and Table S5).

Using a different number of components might induce some degree of variation in model accuracies, although we used the cross-validation (CV) procedure. In addition to the CV-optimized number of components, model calibration and validation were repeated by using a fixed number of components (Table S6, Table S7 and Table S8). Results showed that the first derivative reflectance yielded the highest kappa coefficients, followed by the CR reflectance and the original reflectance (Fig. S3). The SNV reflectance did not yield improvement compared to the original reflectance data, suggesting that the SNV process may mask subtle spectral responses subjected to individual metals. Overall, PLS-DA models based on the first derivative reflectance produced the best classifications, which also suggests that heavy metals have induced complicated effects on leaf biochemical and structural properties that lead to light absorption changes/shifts over the full spectrum.

First derivative spectra of leaves have been proven to be effective in eliminating background signals and for resolving overlapping spectral features (Demetriades-Shah et al., 1990), which is useful to detect plant stresses or estimate pigment changes

(Rundquist et al., 1996; Smith et al., 2004). Also, first derivative reflectance has better discrimination power compared to the original reflectance by characterizing the rate of change of reflectance with respect to wavelengths (Bao et al., 2013; Lassalle et al., 2018; Smith et al., 2004). Typically, derivative analysis may facilitate the detection of changes that might be masked in the original spectra by the presence of plant intrinsic co-variations (Horler et al., 1983). For instance, derivative spectra in the visible region may enable to detect subtle changes in leaf pigment balance associated with physiological disorders or vegetation types (Bandaru et al., 2016; Demetriades-Shah et al., 1990; Pu, 2011).

Derivative analysis can be particularly useful for remotely bio-monitoring heavy metal using reflectance spectra measured from above the vegetation canopy (Wang et al., 2018). Canopy spectra first derivatives eliminate the additive noises (baseline shifts) induced by illumination instability, canopy structural or soil background influences (Demetriades-Shah et al., 1990; Gnyep et al., 2014; Kochubey and Kazantsev, 2012; Pu, 2011), thereby improving the accuracy for quantification of canopy biochemical or physiological changes (Jin and Wang, 2016; O'Connell et al., 2014). Moreover, PLS modeling further facilitates the use of features of the full derivative spectrum for the characterization of vegetation undergoing changes or stresses.

Apparently, PLS-DA models for Pb-contamination classifications exclusively produced higher kappa values than for Cd

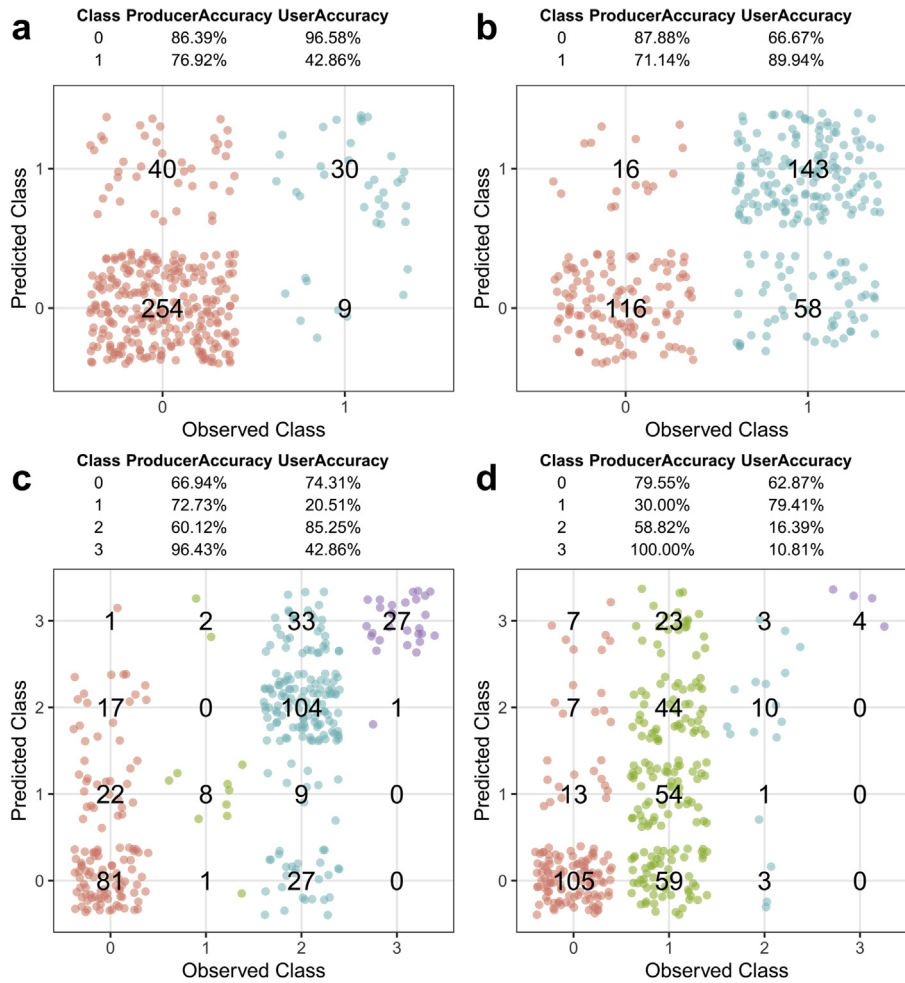


Fig. 5. Predicted versus observed classes for (a) Cd binary classification, (b) Pb binary classification, (c) Cd × Pb classification and (d) Pb multi-class classification. Here the first derivative reflectance data were used for (a), (b) and (c), the original reflectance were used for (d). Numbers indicate the confusion matrix of classification.

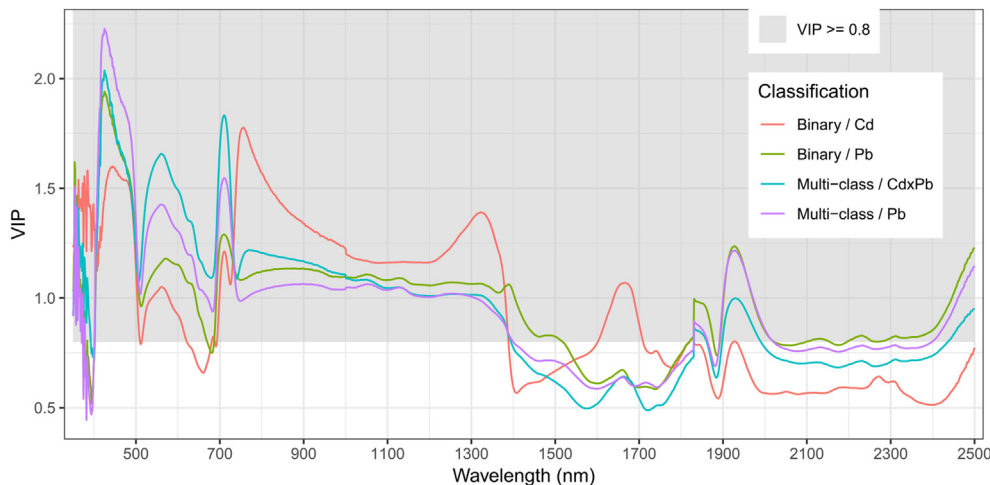


Fig. 6. The variable importance in projection (VIP) scores for the spectral-based PLS-DA models for binary classification for Cd and Pb contamination, and for multi-class classification of Pb and Cd x Pb contamination. VIP ≥ 0.8 highlights the spectral bands contributing significantly to the PLS-DA models.

contamination classifications, across different cases of spectra-preprocessing methods, model calibration (Fig. S3a) and validation (Fig. S3b), as well as when using a subset of VIP-bands (Fig. S3c). This can be attributed to the data imbalance between

the Cd- and Pb-contamination levels, which, however, shows a great promise of the proposed approach for spectroscopic detection of elevated soil heavy metals, given that a diverse set of observations are used for model calibration.

4. Conclusions

This study used *T. tomentosa* trees growing in three European cities as bio-indicators of soil heavy metal contamination, and evaluated whether tree spectra responses were able to reflect the elevated metal concentrations. Results showed that elevated soil Cd and Pb concentrations led to decrease in the leaf mass per area (LMA) and the chlorophyll *a* to *b* ratio (Chla:Chlb), while no significant reduction in leaf total chlorophyll (Chl) and the maximal PSII photochemical efficiency (Fv/Fm). Soil Pb contamination was severer and showed more pronounced effect on LMA, Fv/Fm, Chl and Chla:Chlb than did the Cd contamination in the studied sites.

Cd and Pb contamination induced specific changes in leaf reflectance and the reflectance first derivatives, particularly in the red-edge spectral region. Partial least squares discriminant analysis (PLS-DA) models calibrated using leaf reflectance showed promise for detecting soil Cd and Pb contamination in urban areas. PLS-DA models based on reflectance first derivatives allowed for the best classification of Cd and Pb contamination. This study shows that elevated soil heavy metals can be monitored by measuring leaf spectra of trees. This holds great potential for mapping urban heavy metal contamination by measuring urban vegetation using high-resolution spectrometers onboard airborne or drone platforms. Future work should investigate whether our findings can be extrapolated to broader scales by using canopy level reflectance data and a diverse set of plant species as bio-indicators. Multi-temporal investigations of the quantitative relationships between the practical content of heavy metals in leaves and reflectance spectroscopic measures are also needed to understand metal translocation from soil to vegetation and for dynamic bio-monitoring of heavy metal contamination.

Declarations of interest

None.

Acknowledgements

This research was funded through the 2015–2016 BiodivERsA COFUND call for research proposals, with the national funders BELSPO (BE), FWO (BE), and FCT (PT) through the project UID/Multi/50016/2013. We thank Remi Chevalier, the greenery service of the Cities of Leuven, Porto (Câmara Municipal do Porto) and Strasbourg for their assistance in fieldwork and measurements. The authors thank Remi Chevalier and Yasmin Vanbrabant for their assistance in chlorophyll analysis.

Appendix A. Supplementary data

Supplementary data to this article can be found online at <https://doi.org/10.1016/j.envpol.2018.09.053>.

References

- O'Connell, J.L., Byrd, K.B., Kelly, M., 2014. Remotely-sensed indicators of N-related biomass allocation in *schoenoplectus acutus*. *PLoS One* 9. <https://doi.org/10.1371/journal.pone.0090870>.
- Amer, M., Tyler, A., Fouda, T., Hunter, P., Elmetwalli, A., Wilson, C., VALLEJO-MARIN, Mario, 2017. Spectral characteristics for estimation heavy metals accumulation in wheat plants and grain. *Sci. Pap. Ser. Manag. Econ. Eng. Agric. Rural Dev.* 17, 47–55.
- Andersson, M., Ottesen, R.T., Langedal, M., 2010. Geochemistry of urban surface soils — monitoring in Trondheim, Norway. *Geoderma* 156, 112–118. <https://doi.org/10.1016/j.geoderma.2010.02.005>.
- Bandaru, V., Daughtry, C.S., Codling, E.E., Hansen, D.J., White-Hansen, S., Green, C.E., 2016. Evaluating leaf and canopy reflectance of stressed rice plants to monitor arsenic contamination. *Int. J. Environ. Res. Publ. Health* 13. <https://doi.org/10.3390/ijerph13060606>.
- Bao, J., Chi, M., Benediktsson, J.A., 2013. Spectral derivative features for classification of hyperspectral remote sensing images: experimental evaluation. *IEEE J. Sel. Top. Appl. Earth Obs. Remote Sens.* 6, 594–601. <https://doi.org/10.1109/JSTARS.2013.2237758>.
- Barceló, J., Poschenrieder, C., 1990. Plant water relations as affected by heavy metal stress: a review. *J. Plant Nutr.* 13, 1–37. <https://doi.org/10.1080/01904169009364057>.
- Bates, D., Mächler, M., Bolker, B., Walker, S., 2015. Fitting linear mixed-effects models using lme4. *J. Stat. Software* 67, 1–48. <https://doi.org/10.18637/jss.v067.i01>.
- Clevers, J.G.P.W., Kooistra, L., Salas, E.A.L., 2004. Study of heavy metal contamination in river floodplains using the red-edge position in spectroscopic data. *Int. J. Rem. Sens.* 25, 3883–3895. <https://doi.org/10.1080/01431160310001654473>.
- Demetriades-Shah, T.H., Steven, M.D., Clark, J.A., 1990. High resolution derivative spectra in remote sensing. *Remote Sens. Environ.* 33, 55–64. [https://doi.org/10.1016/0034-4257\(90\)90055-Q](https://doi.org/10.1016/0034-4257(90)90055-Q).
- Doganlar, Z.B., Doganlar, O., Erdogan, S., Onal, Y., 2012. Heavy metal pollution and physiological changes in the leaves of some shrub, palm and tree species in urban areas of Adana, Turkey. *Chem. Speciat. Bioavailab.* 24, 65–78. <https://doi.org/10.3184/095422912X13338055043100>.
- European Commission, 2006. Commission Staff Working Document - Document Accompanying the Communication from the Commission to the Council, the European Parliament, the European Economic and Social Committee and the Committee of the Regions - Thematic Strategy for Soil Protection - Impact Assessment of the Thematic Strategy on Soil Protection (COM(2006)231 Final) [SEC(2006)1165]. Commission of the European Communities, Brussels.
- Gallagher, F.J., Pechmann, I., Bogden, J.D., Grabosky, J., Weis, P., 2008. Soil metal concentrations and productivity of *Betula populifolia* (gray birch) as measured by field spectrometry and incremental annual growth in an abandoned urban Brownfield in New Jersey. *Environ. Pollut.* 156, 699–706. <https://doi.org/10.1016/j.envpol.2008.06.013>.
- Giulia, M., Lucia, S., Carmen, A., 2013. Heavy metal accumulation in leaves affects physiological performance and litter quality of *Quercus ilex* L. *J. Plant Nutr. Soil Sci.* 176, 776–784. <https://doi.org/10.1002/jpln.201200053>.
- Gnyp, M.L., Miao, Y., Yuan, F., Ustin, S.L., Yu, K., Yao, Y., Huang, S., Bareth, G., 2014. Hyperspectral canopy sensing of paddy rice aboveground biomass at different growth stages. *Field Crop. Res.* 155, 42–55. <https://doi.org/10.1016/j.fcr.2013.09.023>.
- Ho, Y.B., 1990. *Ulva lactuca* as bioindicator of metal contamination in intertidal waters in Hong Kong. *Hydrobiologia* 203, 73–81. <https://doi.org/10.1007/BF00005615>.
- Holt, E.A., Miller, S.W., 2010. Bioindicators: using organisms to measure environmental impacts | learn science at scitable. *Nat. Educ. Knowl.* 3, 8.
- Horler, D.N.H., Barber, J., Barringer, A.R., 1980. Effects of heavy metals on the absorbance and reflectance spectra of plants. *Int. J. Rem. Sens.* 1, 121–136. <https://doi.org/10.1080/01431168008547550>.
- Horler, D.N.H., Dockray, M., Barber, J., 1983. The red edge of plant leaf reflectance. *Int. J. Rem. Sens.* 4, 273–288. <https://doi.org/10.1080/01431168308948546>.
- Huang, M., Zhu, H., Zhang, J., Tang, D., Han, X., Chen, L., Du, D., Yao, J., Chen, K., Sun, J., 2017. Toxic effects of cadmium on tall fescue and different responses of the photosynthetic activities in the photosystem electron donor and acceptor sides. *Sci. Rep.* 7. <https://doi.org/10.1038/s41598-017-14718-w>.
- Jin, J., Wang, Q., 2016. Hyperspectral indices based on first derivative spectra closely trace canopy transpiration in a desert plant. *Ecol. Inf.* 35, 1–8. <https://doi.org/10.1016/j.ecoinf.2016.06.004>.
- Kastori, R., Plesničar, M., Sakač, Z., Panković, D., Arsenijević-Maksimović, I., 1998. Effect of excess lead on sunflower growth and photosynthesis. *J. Plant Nutr.* 21, 75–85. <https://doi.org/10.1080/01904169809365384>.
- Khavanin Zadeh, A.R., Veroustraete, F., Buytaert, J.A.N., Dirckx, J., Samson, R., 2013. Assessing urban habitat quality using spectral characteristics of Tilia leaves. *Environ. Pollut.* 178, 7–14. <https://doi.org/10.1016/j.envpol.2013.02.021>.
- Kochubey, S.M., Kazantsev, T.A., 2012. Derivative vegetation indices as a new approach in remote sensing of vegetation. *Front. Earth Sci.* 6, 188–195. <https://doi.org/10.1007/s11707-012-0325-z>.
- Kooistra, L., Leuven, R.S.E.W., Wehrens, R., Nienhuis, P.H., Buydens, L.M.C., 2003. A comparison of methods to relate grass reflectance to soil metal contamination. *Int. J. Rem. Sens.* 24, 4995–5010. <https://doi.org/10.1080/0143116031000080769>.
- Kooistra, L., Salas, E.A.L., Clevers, J.G.P.W., Wehrens, R., Leuven, R.S.E.W., Nienhuis, P.H., Buydens, L.M.C., 2004. Exploring field vegetation reflectance as an indicator of soil contamination in river floodplains. *Environ. Pollut.* 127, 281–290. [https://doi.org/10.1016/S0269-7491\(03\)00266-5](https://doi.org/10.1016/S0269-7491(03)00266-5).
- Kovarik, W., 2005. Ethyl-leaded gasoline: how a classic occupational disease became an international public health disaster. *Int. J. Occup. Environ. Health* 11, 384–397. <https://doi.org/10.1179/oeh.2005.11.4.384>.
- Kumar, L., Schmidt, K., Dury, S., Skidmore, A., 2001. Imaging spectrometry and vegetation science. In: van der Meer, F.D., De Jong, S.M. (Eds.), *Imaging Spectrometry - Basic Principles and Prospective Applications, Remote Sensing and Digital Image Processing*. Springer Netherlands, Dordrecht, pp. 111–155. https://doi.org/10.1007/978-0-306-47578-8_5.
- Lassalle, G., Credoz, A., Hédacq, R., Fabre, S., Dubucq, D., Elger, A., 2018. Assessing soil contamination due to oil and gas production using vegetation hyperspectral reflectance. *Environ. Sci. Technol.* 52, 1756–1764. <https://doi.org/10.1021/acs.est.7b04618>.
- Lenth, R.V., 2016. Least-squares means: the R package lsmeans. *J. Stat. Software* 69,

- 1–33. <https://doi.org/10.18637/jss.v069.i01>.
- Li, X., Poon, C., Liu, P.S., 2001. Heavy metal contamination of urban soils and street dusts in Hong Kong. *Appl. Geochem.* 16, 1361–1368. [https://doi.org/10.1016/S0883-2927\(01\)00045-2](https://doi.org/10.1016/S0883-2927(01)00045-2).
- Lichtenthaler, H.K., 1987. [34] Chlorophylls and carotenoids: pigments of photosynthetic biomembranes. *Methods in Enzymology, Plant Cell Membranes*. Academic Press, pp. 350–382. [https://doi.org/10.1016/0076-6879\(87\)48036-1](https://doi.org/10.1016/0076-6879(87)48036-1).
- Liedekerke, M. van, Prokop, G., Rabl-Berger, S., Kibblewhite, M., Louwagie, G., European Commission, Joint Research Centre, Institute for Environment and Sustainability, 2014. *Progress in the Management of Contaminated Sites in Europe*. Publications Office of the European Union, Luxembourg.
- Manios, T., Stentiford, E.I., Millner, P.A., 2003. The effect of heavy metals accumulation on the chlorophyll concentration of *Typha latifolia* plants, growing in a substrate containing sewage sludge compost and watered with metaliferous water. *Ecol. Eng.* 20, 65–74. [https://doi.org/10.1016/S0925-8574\(03\)00004-1](https://doi.org/10.1016/S0925-8574(03)00004-1).
- MEF, 2007. *Government Decree on the Assessment of Soil Contamination and Remediation Needs (No. 214/2007)*. Ministry of the Environment, Finland.
- Nie, J., Liu, Y., Zeng, G., Zheng, B., Tan, X., Liu, H., Xie, J., Gan, C., Liu, W., 2016. Cadmium accumulation and tolerance of *Macleaya cordata*: a newly potential plant for sustainable phytoremediation in Cd-contaminated soil. *Environ. Sci. Pollut. Res.* 23, 10189–10199. <https://doi.org/10.1007/s11356-016-6263-7>.
- Ouyang, H., Kong, X., He, W., Qin, N., He, Q., Wang, Y., Wang, R., Xu, F., 2012. Effects of five heavy metals at sub-lethal concentrations on the growth and photosynthesis of *Chlorella vulgaris*. *Chin. Sci. Bull.* 57, 3363–3370. <https://doi.org/10.1007/s11434-012-5366-x>.
- Panagos, P., Van Liedekerke, M., Yigini, Y., Montanarella, L., 2013. Contaminated sites in Europe: review of the current situation based on data collected through a European network. *J. Environ. Public Health* 2013, 11. <https://doi.org/10.1155/2013/158764>.
- Pandit, C.M., Filippelli, G.M., Li, L., 2010. Estimation of heavy-metal contamination in soil using reflectance spectroscopy and partial least-squares regression. *Int. J. Rem. Sens.* 31, 4111–4123. <https://doi.org/10.1080/01431160903229200>.
- Parmar, T.K., Rawtani, D., Agrawal, Y.K., 2016. Bioindicators: the natural indicator of environmental pollution. *Front. Life Sci.* 9, 110–118. <https://doi.org/10.1080/21553769.2016.1162753>.
- Poggio, L., Vrščaj, B., Schulin, R., Hepperle, E., Ajmone Marsan, F., 2009. Metals pollution and human bioaccessibility of topsoils in Grugliasco (Italy). *Environ. Pollut.* 157, 680–689. <https://doi.org/10.1016/j.envpol.2008.08.009>.
- Pourkhabbaz, A., Rastin, N., Olbrich, A., Langenfeld-Heyser, R., Polle, A., 2010. Influence of environmental pollution on leaf properties of urban plane trees, *platanus orientalis* L. *Bull. Environ. Contam. Toxicol.* 85, 251–255. <https://doi.org/10.1007/s00128-010-0047-4>.
- Pu, R., 2011. Detecting and mapping invasive plant species by using hyperspectral data. In: Thenkabail, P.S., Lyon, J.G., Huete, A. (Eds.), *Hyperspectral Remote Sensing of Vegetation*. CRC Press, Boca Raton, FL, p. 447.
- R Core Team, 2016. *R: a Language and Environment for Statistical Computing*. R Foundation for Statistical Computing, Vienna, Austria.
- Rohart, F., Gautier, B., Singh, A., Cao, K.-A.L., 2017. mixOmics: an R package for 'omics feature selection and multiple data integration. *bioRxiv* 108597. <https://doi.org/10.1101/108597>.
- Rosipal, R., Krämer, N., 2006. Overview and recent advances in partial least squares. In: *Subspace, Latent Structure and Feature Selection*, Lecture Notes in Computer Science. Springer, Berlin, Heidelberg, pp. 34–51. https://doi.org/10.1007/11752790_2.
- Rosso, P.H., Pushnik, J.C., Lay, M., Ustin, S.L., 2005. Reflectance properties and physiological responses of *Salicornia virginica* to heavy metal and petroleum contamination. *Environ. Pollut.* 137, 241–252. <https://doi.org/10.1016/j.envpol.2005.02.025>.
- Rundquist, D.C., Han, L., Schalles, J.F., Peake, J.S., 1996. Remote measurement of algal chlorophyll in surface waters: the case for the first derivative of reflectance near 690 nm. *Photogramm. Eng. Rem. Sens.* 62, 195–200.
- Sawidis, T., Breuste, J., Mitrovic, M., Pavlovic, P., Tsigaridas, K., 2011. Trees as bio-indicator of heavy metal pollution in three European cities. *Environ. Pollut.* 159, 3560–3570. <https://doi.org/10.1016/j.envpol.2011.08.008>.
- Shen, J., Song, L., Müller, K., Hu, Y., Song, Y., Yu, W., Wang, H., Wu, J., 2016. Magnesium alleviates adverse effects of lead on growth, photosynthesis, and ultrastructural alterations of *Torreya grandis* seedlings. *Front. Plant Sci.* 7. <https://doi.org/10.3389/fpls.2016.01819>.
- Shi, G., Cai, Q., 2009. Leaf plasticity in peanut (*Arachis hypogaea* L.) in response to heavy metal stress. *Environ. Exp. Bot.* 67, 112–117. <https://doi.org/10.1016/j.envexpbot.2009.02.009>.
- Shi, T., Chen, Y., Liu, Y., Wu, G., 2014. Visible and near-infrared reflectance spectroscopy—an alternative for monitoring soil contamination by heavy metals. *J. Hazard Mater.* 265, 166–176. <https://doi.org/10.1016/j.jhazmat.2013.11.059>.
- Smith, K.L., Steven, M.D., Colls, J.J., 2004. Use of hyperspectral derivative ratios in the red-edge region to identify plant stress responses to gas leaks. *Remote Sens. Environ.* 92, 207–217. <https://doi.org/10.1016/j.rse.2004.06.002>.
- Tóth, G., Hermann, T., Da Silva, M.R., Montanarella, L., 2016. Heavy metals in agricultural soils of the European Union with implications for food safety. *Environ. Int.* 88, 299–309. <https://doi.org/10.1016/j.envint.2015.12.017>.
- Vince, T., Szabó, G., Csoma, Z., Sándor, G., Szabó, S., 2014. The spatial distribution pattern of heavy metal concentrations in urban soils — a study of anthropogenic effects in Berehove, Ukraine. *Cent. Eur. J. Geosci.* 6, 330–343. <https://doi.org/10.2478/s13533-012-0179-7>.
- Wang, F., Gao, J., Zha, Y., 2018. Hyperspectral sensing of heavy metals in soil and vegetation: feasibility and challenges. *ISPRS J. Photogrammetry Remote Sens.* 136, 73–84. <https://doi.org/10.1016/j.isprsjprs.2017.12.003>.
- Wei, B., Yang, L., 2010. A review of heavy metal contaminations in urban soils, urban road dusts and agricultural soils from China. *Microchem. J.* 94, 99–107. <https://doi.org/10.1016/j.microc.2009.09.014>.
- Wold, S., Sjöström, M., Eriksson, L., 2001. PLS-regression: a basic tool of chemometrics. *Chemom. Intell. Lab. Syst., PLS Methods* 58, 109–130. [https://doi.org/10.1016/S0169-7439\(01\)00155-1](https://doi.org/10.1016/S0169-7439(01)00155-1).
- Wu, M., Wang, P.-Y., Sun, L.-G., Zhang, J.-J., Yu, J., Wang, Y.-W., Chen, G.-X., 2014. Alleviation of cadmium toxicity by cerium in rice seedlings is related to improved photosynthesis, elevated antioxidant enzymes and decreased oxidative stress. *Plant Growth Regul.* 74, 251–260. <https://doi.org/10.1007/s10725-014-9916-x>.